Proceedings of the Korean Nuclear Society Autumn Meeting
Taejon, Korea, October 2000

Analysis of Thermohydraulic Phenomena in the Hot Pool of KALIMER Design

Yong-Bum Lee, Won Pyo Chang, Young Min Kwon, Kwan Seong Jeong and Dohee Hahn

Korea Atomic Energy Research Institute
KALIMER Technology Development Team
Yusong P.O. Box 105, Taejon, Korea 305-600

Abstract

The SSC-K code is developed at KAERI on the basis of SSC-L originally developed at BNL to analyze loop-type LMR transient. Because the dynamic response of the primary coolant in a pool-type LMR, particularly the hot pool concept, can be quite different from that in the loop-type LMR, the major modifications of SSC-L have been made for the safety analysis of KALIMER. In particular, it is necessary to predict the hot pool coolant temperature distribution with sufficient accuracy to determine the inlet temperature conditions for the IHXs because the temperature distribution of hot pool can alter the overall system response. In this paper two-dimensional hot pool model is developed and is compared to the experimental data. A preliminary evaluation of unprotected loss of heat sink accident for the KALIMER design with updated SSC-K code has been performed and analyzed.

1. Introduction

The Super System Code of KAERI (SSC-K) is developed at Korea Atomic Energy Research Institute (KAERI) on the basis of SSC-L originally developed at BNL to analyze loop-type LMR (Liquid Metal Reactor) transient [1]. Because the dynamic response of the primary coolant in a pool-type LMR, particularly the hot pool concept, can be quite different from that in the loop-type LMR, the major modifications of SSC-L have been made for the safety analysis of KALIMER [2]. The major difference between KALIMER and general loop-type LMRs exists in the primary heat transport system. In KALIMER, all of the essential components composing the primary heat transport system are located within the reactor vessel. They include the reactor, four EM pumps, the primary side of four intermediate heat exchangers, sodium pools, cover gas blanket, and associated pipings. This is contrast to the loop-type LMRs, in which all the primary components are connected via piping to form loops external to the reactor vessel.

During a normal reactor scram, the heat generation is reduced almost instantaneously while the coolant flow rate follows the pump coastdown. This mismatch between power and flow results in a situation where the core flow entering the hot pool is at a lower temperature than the temperature of the bulk pool sodium. This temperature difference leads to thermal stratification. Thermal stratification can occur in the hot pool region if the entering coolant is colder than the existing hot pool coolant and the flow momentum is not large enough to overcome the negative buoyancy force. Since the fluid of hot pool enters IHXs, the temperature distribution of hot pool can alter the overall system response. Hence, it is necessary to predict the pool coolant temperature distribution with sufficient accuracy to determine the inlet temperature conditions for the IHXs and its contribution to the net buoyancy head.

Therefore, in this paper two-dimensional hot pool model is developed instead of existing one-dimensional model to predict the hot pool coolant temperature and velocity distribution more accurately and is applied to the SSC-K code. Also, the comparisons of the model with experimental data are performed and analyzed and a preliminary evaluation of unprotected loss of heat sink (ULOHS) accident for the KALIMER design has been performed with existing one-dimensional and developed two-dimensional hot pool model.

2. General Modeling Description

Figure 1 shows a schematic diagram of SSC-K modeling for KALIMER. KALIMER has only one cover gas space and the IHX outlet is directly connected to cold pool. Since the sodium in the hot pool is separated from the cold pool by insulated barrier in KALIMER, the liquid level in the hot pool is different from that in the cold pool mainly due to hydraulic losses and pump suction heads occurring during flow through the circulation paths. In some accident conditions the liquid in the hot pool is flooded into cold pool and forms a natural circulation flow path. During the loss of heat sink transients, this will provide as a major heat removal mechanism with the passive decay heat removal system. Since the pipes in the primary system exists only between the pump discharge and the core inlet plenum and are submerged in the cold pool, a pipe rupture accident becomes less severe because of a constant back pressure exerted against the coolant flow from break.

2.1 One-Dimensional Hot Pool Model

The core flow in the hot pool is represented by a two-zone model. The hot pool is divided into two perfectly mixing zones determined by the maximum penetration distance of the core flow. This penetration distance is a function of the Froude number of the average core exit flow. The temperature of each zone is

computed from energy balance considerations. The temperature of the upper portion, T_A, will be relatively unchanged; in the lower region, however, T_B will be changed and somewhat between the core exit temperature and the temperature of the upper zone due to active mixing with core exit flow as well as heat transfer with the upper zone. The temperature of upper zone is mainly affected by interfacial heat transfer.

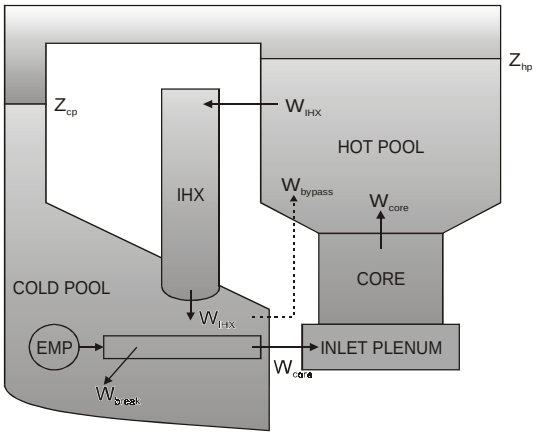

Fig. 1 Schematic of SSC-K modeling for KALIMER

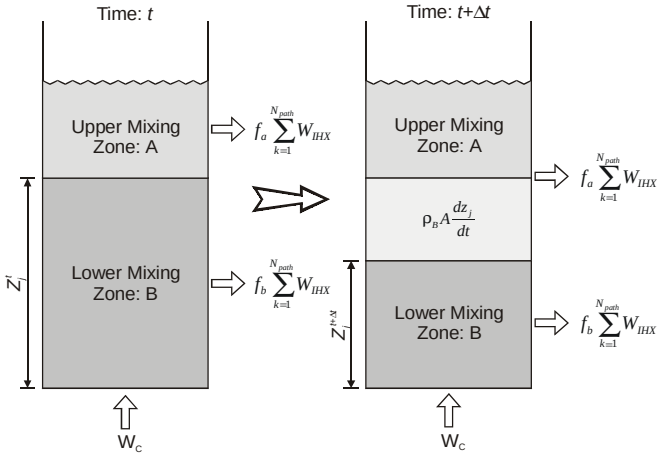

Fig. 2 One-dimensional two-mixing zone model

2.2 Two-Dimensional Hot Pool Model

The previous two-zone model is only applicable to the very slow transitions or steady state conditions. A two-dimensional pool model[3] has been developed to calculate the coolant temperature and velocity profiles in the hot pool. The solution domain is divided into a finite number of quadrilateral control volumes and the discretization of the governing equation is performed following the finite volume approach. The convection terms are approximated by a higher-order bounded scheme HLPA developed by Zhu[4] and the unsteady terms are treated by the backward differencing scheme.

Heat transfer to the wall of the pool is calculated along the wall surface. The governing equations for conservation of mass, momentum, energy, and both turbulent kinetic energy and the rate of turbulent kinetic energy dissipation for the $\kappa-\varepsilon$ turbulence model are made in a generalized coordinate system. In the momentum interpolation method, the Rhie and Chows scheme[5~7] is modified to obtain a converged solution for unsteady flows which is independent of the size of time step and relaxation factors. The momentum equations are solved implicitly at the cell-centered locations in the Rhie and Chows scheme. The SIMPLEC[8] algorithm is used for pressure-velocity coupling, where the momentum equations are implicitly

solved at cell-centered locations[9]. After validation of the stand-alone version of the two-dimensional pool model against the sample problem, it has been coupled with the SSC-K code. Users can select the two-dimensional model or the two-mixing zone model for the hot pool simulation. The detailed governing equations and constitutive equations of two-dimensional hot pool model is described in the author's published paper[3].

3. Comparison Results of the Model with Experimental Data

3.1 Description of MONJU Upper Plenum and Modeling

In order to estimate the accuracy and reliability of the developed model, calculated results are compared with the measured data obtained from the Monju plant 40% power condition trip test. The principal data of plant design and performance are shown in Table 1.

Table 1 Principal design and performance data of Monju

○ Reactor type	Sodium cooled loop-type
○ Thermal power	714MW_t
○ Electric power	280MW_e
○ Fuel material	PuO_2-UO_2
○ Core equivalent diameter	1,790mm
○ Core height	930mm
○ Core Inlet/outlet sodium temperature	397/529℃
○ IHX Inlet/outlet sodium temperature	325/505℃
○ Height of reactor vessel	18m
○ Diameter of reactor vessel	7m
○ Number of loop	3
○ Type of steam generator	Helical coil
○ Steam pressure	12.7MPa
○ Steam temperature	483℃

The structure of upper plenum includes the Upper Internal Structure(UIS), annular space formed by thin thermal liner and reactor vessel wall. The thermal liner has upper and lower flow holes, and the upper plenum is covered by inert gas. Those structures that comprises upper plenum are schematically shown in Fig.3. The UIS is installed at the center of reactor vessel and its shape is cylindrical. The thermal liner is located 21.3cm inside the reactor vessel and it forms annular space with reactor vessel wall which provides over flow path. And also there are two flow paths at two elevation levels, lower and upper, through the reactor vessel liner.

Lower and upper flow paths consist of 48 and 24 holes respectively whose diameter is 96mm and is located at 0.65m and 1.62m from top of the core, respectively.

The coolant coming from the core exit enters the plenum through the bottom section and then flows in the three flow paths. The coolant leaving each flow hole and over flow path exits the reactor vessel outlet nozzle and transfers heat to the secondary side of intermediate heat exchanger(IHX). The calculated model is a two-dimensional cylindrical geometry with a cell partition of 26×15, as shown in Fig.4.

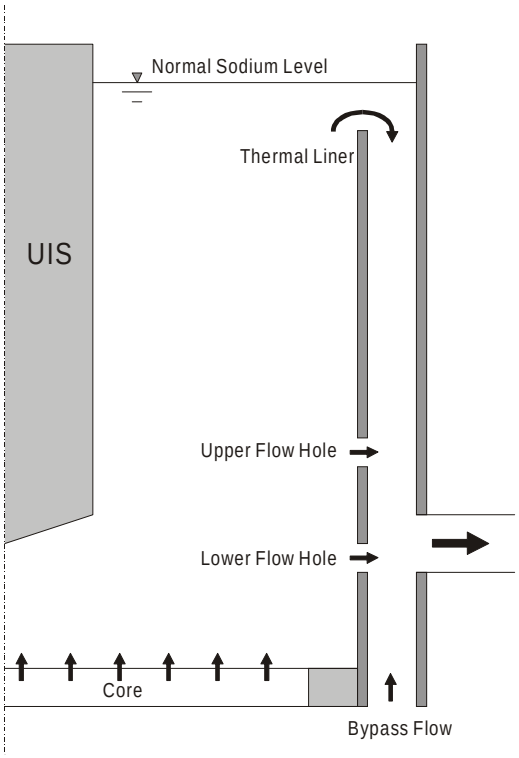

Fig. 3 Configuration of MONJU upper plenum

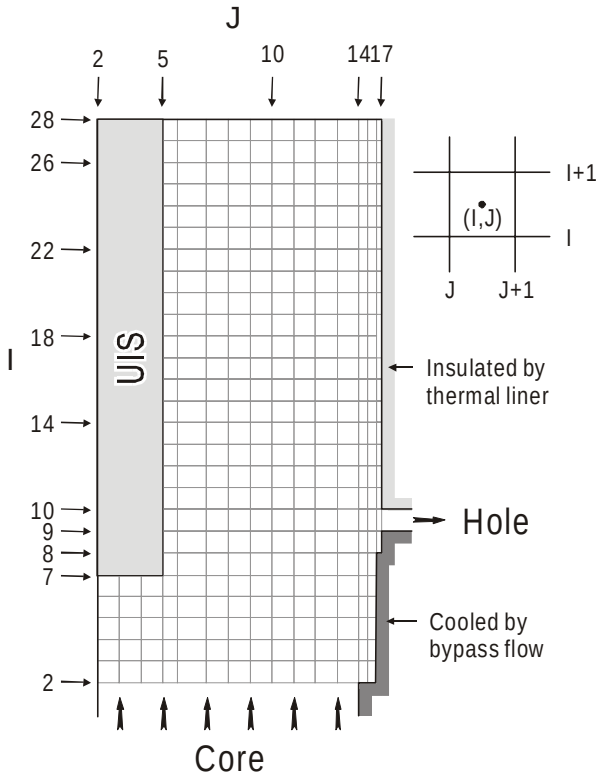

Fig. 4 Mesh arrangement of MONJU upper plenum

3.2 Analysis Results

Figure 5 and 6 show the hot pool inlet temperature and flowrate after scram[10]. The comparisons of axial temperature distribution in upper plenum between calculation and measurement are given in Fig.7. In the figures, the calculated temperature distributions are shown in the near region of reactor thermal liner at steady state and transient condition. In the Monju plant, 38 thermocouples are installed in the near thermal liner in axial direction from normal sodium level to the top of the reactor core.

As shown in Fig.7(a), in the steady state condition, the calculated results agree

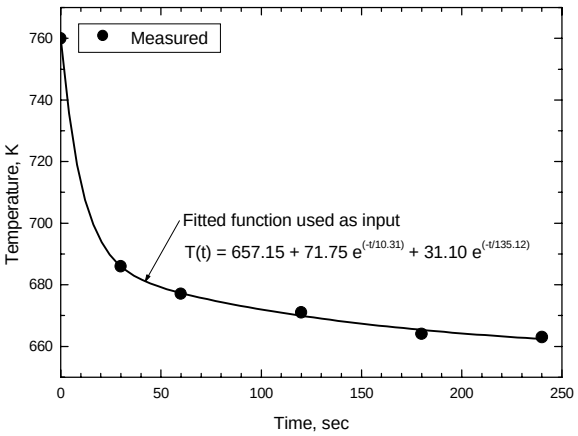

Fig. 5 Hot pool inlet temperature

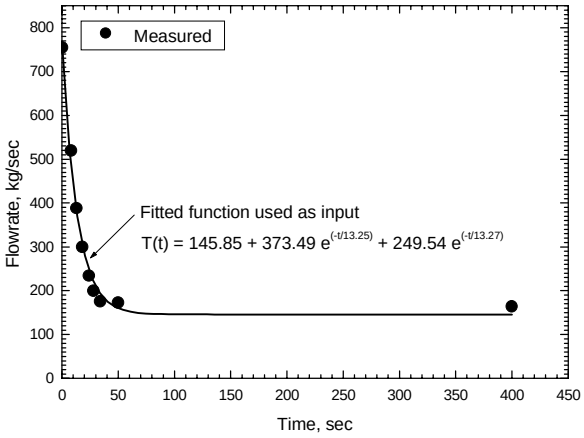

Fig. 6 Hot pool inlet flowrate

well with measured data from normal sodium level to around flow hole, 4 meter below from sodium level, but there is some temperature differences below the flow hole. The flow hole is located at about 4m below from the normal sodium level. At 30, 60 and 120 seconds after scram, it can be seen that the calculated results show similar tendency with that of steady state but temperature difference in the near flow hole is gradually decreased with time. It seems that the temperature difference deviation is caused by bypass flow cooling. As shown in Fig.3, there is heat transfer between upper plenum sodium and bypass flow in the near region of thermal liner and below flow hole region. Therefore, the measured sodium temperatures below flow hole are lower than that of calculated ones. In the present model, there is no bypass flow model. As time goes by, the temperature difference between core exit sodium and bypass flow decreases and then the predicted temperatures below flow hole comes close to the measured ones. At 180 and 240 seconds after scram, the calculated results are in good agreement with measured data. As a results, using present 2-dimensional upper plenum model, upper plenum exit sodium temperature can be predicted well.

An emergency shutdown causes a sharp temperature reduction at core exit. These temperature variations result in density change which may affect flow conditions, particularly in regions of low flow velocity. As results of these phenomena, hot fluid is left in the lower region and density interface brought by the temperature difference exists between two temperature regions. Figure 8 shows the variation of the sodium temperature in upper plenum at steady state and 10, 30, 60, 90, 120, 180 and 240 seconds after scram. After scram condition, since the core exit temperature is decreased abruptly and it can be seen the thermal stratification phenomena in upper plenum. As shown in Fig.8, since there is heat transfer from hot region to cold region during transient, the density interface gradually moves up in the upper plenum. According to the study by Tomonari[11], it is known that the rising speed of the density interface is inversely proportional to the Ri number and is proportional to the Pr number.

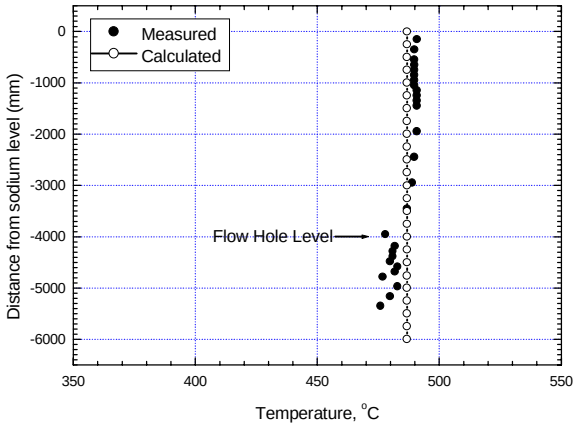

(a) 0 sec

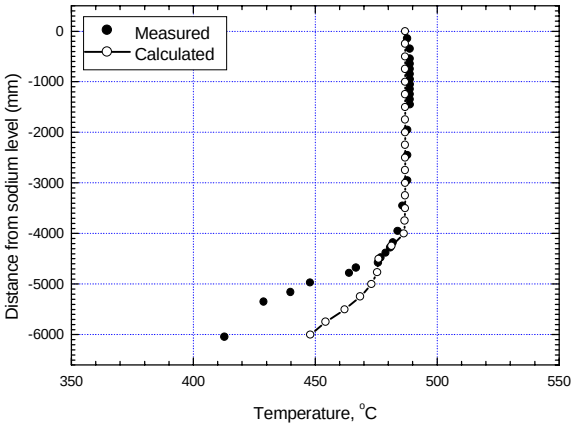

(b) 30 sec

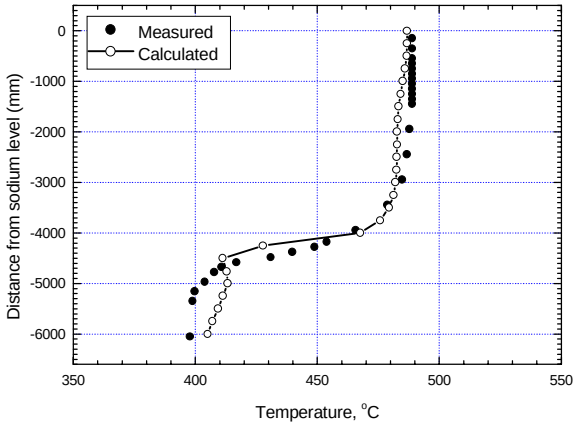

(c) 120 sec

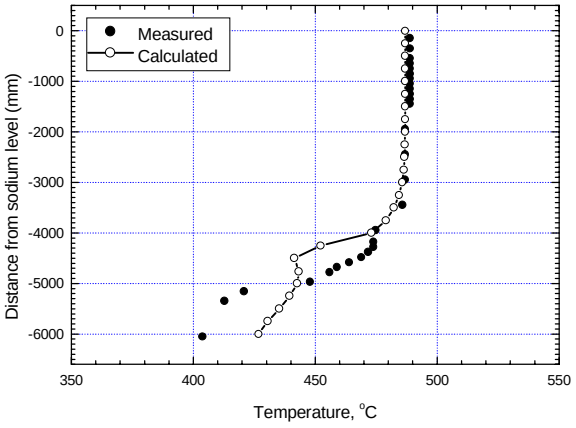

(d) 60 sec

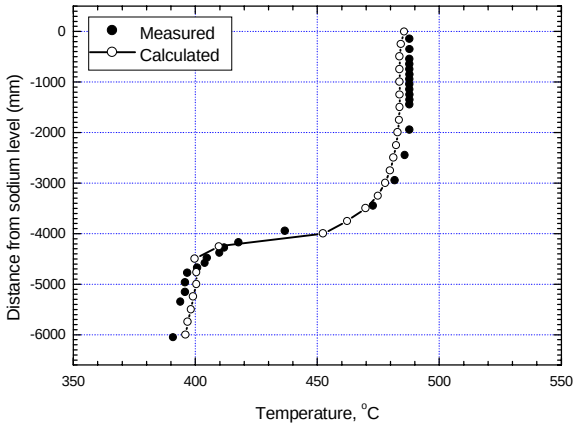

(e) 180 sec

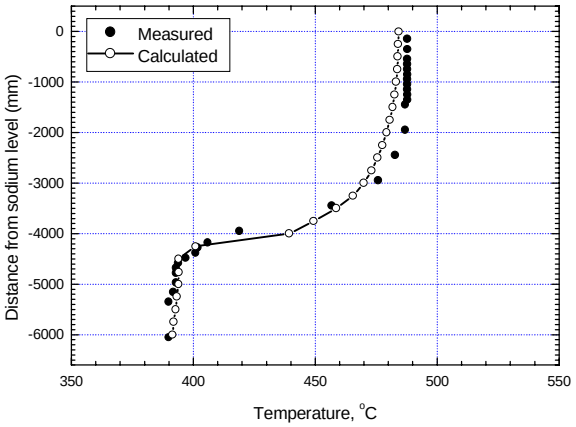

(f) 240 sec

Fig. 7 Axial temperature distributions in the upper plenum

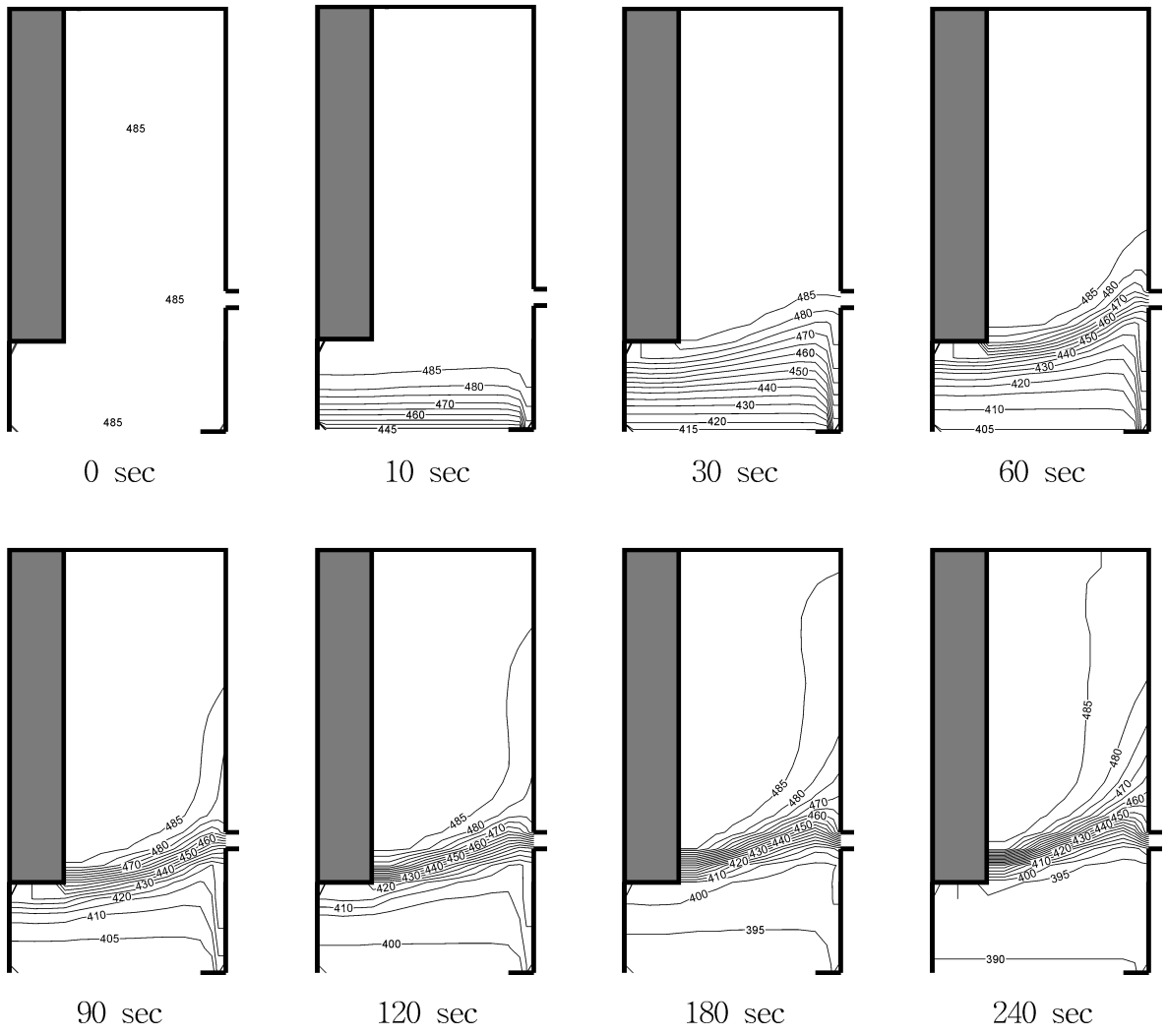

Fig. 8 Radial temperature distributions in the upper plenum

4. Analysis of ULOHS accident in KALIMER Design

4.1 Description of KALIMER Hot Pool and Modeling

The KALIMER reactor internal structures are composed of the core support structure, the inlet plenum, the support barrel, the reactor baffle, the reactor baffle plate, the separation plate, the flow guide, the EMP nozzle, the inlet pipe, and the radiation shield structure. As shown in Fig.9, the annulus type internal structure called as the reactor baffle annulus, which is composed of the reactor baffle, the support barrel, the reactor baffle plate, and the separation plate, is provided to mitigate the large thermal gradients generated between hot and cold sodium boundaries. The temperature of stagnant sodium in the reactor baffle annulus is steadily stratified at all operating conditions and will significantly reduce the thermal stresses of boundary regions of hot and cold sodium.

A upper internal structure(UIS) is attached to rotating plug installed on the reactor head and cantilevered downward into the reactor hot pool. Its bottom end is located above the top of the core assemblies during normal operation. The principal function of UIS is to support the control rod drivelines and to support the core instrument drywell. The calculated model is a two-dimensional cylindrical geometry with a cell partition of 48×12, as shown in Fig.10.

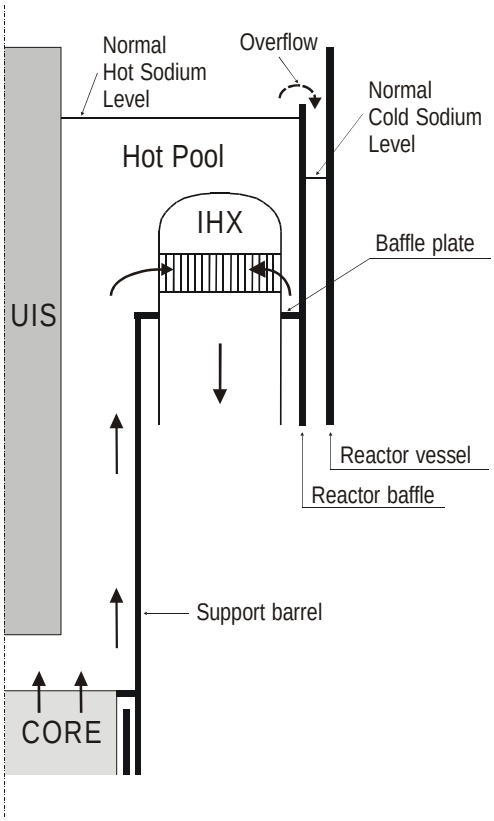

Fig. 9 Configuration of KALIMER hot pool

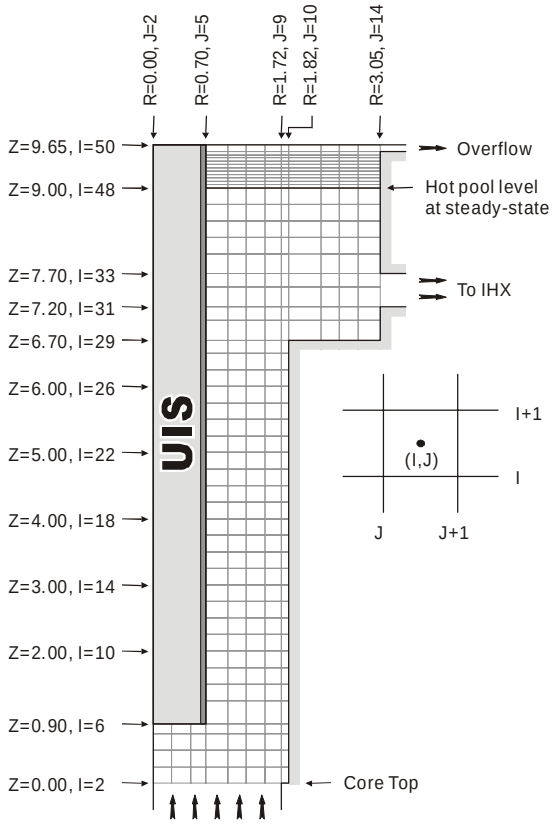

Fig. 10 Mesh arrangement of KALIMER hot pool

4.2 Unprotected Loss of Heat Sink Accident

The loss of heat sink accident starts with a sudden loss of the normal heat removal by a sudden stoppage of the IHTS(Intermediate Heat transport System) flow. Since the natural circulation in the IHTS has been ignored, this event is similar to a complete loss of coolant in the IHTS, as might happen for the case of sodium water reaction in the steam generator or the pipe rupture. All of the heat generated is then retained in the primary vessel and this event would normally be terminated by a reactor scram due to high core temperature.

The primary pump, which is also a heat source, continues to operate at the rated condition until tripped by the plant protection system, a safety grade system to open the pump breakers if the primary cold leg temperature exceeds the predetermined

limit. However, the primary pumps are conservatively assumed to operate at rated condition during the course of event.

Since PSDRS(Passive Decay Heat Removal System) is the only safety-grade heat removal system for KALIMER, it is necessary to closely scrutinize its potential failure modes. Degradation in the system performance is possible and partial failures are also conceivable. The failure mode that seems most significant would be blockage of the air-flowing duct. However, the four independent air-flowing ducts are very large and less probable to be fully blocked, except via a massive earthquake or sabotage. Current analysis has been performed for the case with PSDRS heat removal.

4.3 Analysis Results

The loss of heat sink is assumed to occur at 0 sec. After the initiation of the accident, the heat generation in the core drops rapidly due to a strong negative reactivity in early time of accident as shown in Fig.11. The core power decreases to the level of about 11.3MWt at 5000 seconds, which corresponds to approximately 2.9% of the normal power. Since the primary pumps are running, sufficient head between the hot and cold pool is developed and, thus, the core flowrate keeps almost 92% of the normal flow as shown in Fig.12.

The loss of cooling in IHX leads to rapid increase of the cold pool temperature within a short period of time. As shown in Fig.13, the cold pool temperature reaches almost the same value as that of the hot pool within 500 sec. Thereafter, the hot pool temperature increases very slowly, because of large heat capacity of sodium in the pool. The hot pool level rises because of the volume expansion of the hot pool sodium as shown in Fig.14. At 1798 sec the hot pool level reaches to the top of the reactor baffle and then overflow begins. After beginning of the overflow, the heat removal by PSDRS increases rapidly since the cold pool level increases and the contact area between reactor vessel and cold pool sodium increases accordingly.

Figures 17 and 18 show the variation of temperature and velocity profiles in the hot pool at steady state and transient during the accident. Before beginning of the overflow the flow path is formed from core exit to the hot pool and then, to IHX shell side. However, after beginning of the overflow the flow path is formed from core exit to the cold pool through the hot pool dominantly.

As a result from the present simulation, it is noted that the heat capacity of hot pool sodium is a major factor for keeping coolant subcooling during the accident and the overflow from the hot pool to cold pool accelerates the decay heat removal by PSDRS.

5. Conclusions

It is necessary to predict the hot pool sodium temperature distribution with sufficient accuracy to determine the core inlet temperature conditions. Therefore, two-dimensional hot pool model is developed and applied to SSC-K pool-type LMR transient analysis computer code. From comparative results of predictions using the developed two-dimensional model and the ecpermental data, some conclusions including recommendations for future works are as follows:

① Using 2-dimensional hot pool model, the hot pool temperature and velocity distributions can be predicted well and, especially, axial temperature distribution is in good agreement with experimental data.

② From the analysis of the ULOHS accident in KALIMER design, it is concluded that the heat capacity of the hot pool sodium is a major factor for keeping coolant subcooling during accident.

③ The overflow from the hot pool to cold pool accelerates the decay heat removal by PSDRS.

④ The KALIMER design has the inherent safety characteristics and is capable of accomodating unprotected accidents, which is mainly due to the reactivity feedback effects and pool type reactor design.

⑤ More investigation through both analytical and experimental efforts are necessary for the verification and validation of the present hot pool model and also SSC-K computer code.

Acknowledgement

This work was performed under the long-term Nuclear R&D Program sponsored by the Ministry of Science and Technology.

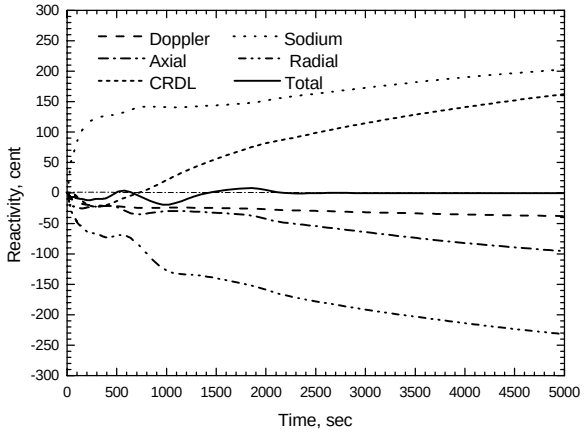

Fig. 11 Reactivity

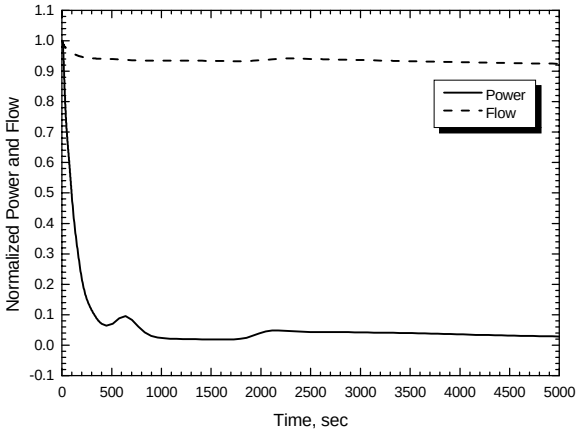

Fig. 12 Normalized power and flow

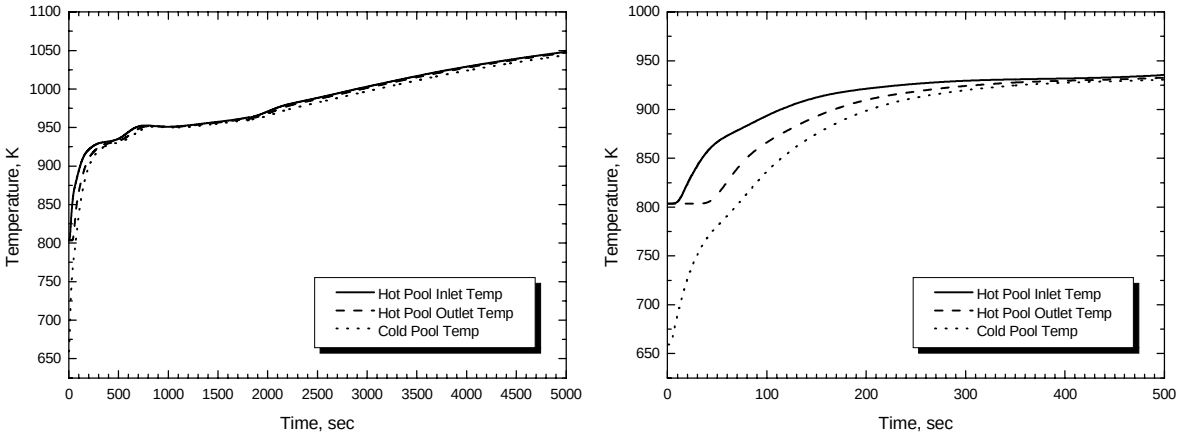

Fig. 13 Temperature variations of the hot and cold pool sodium

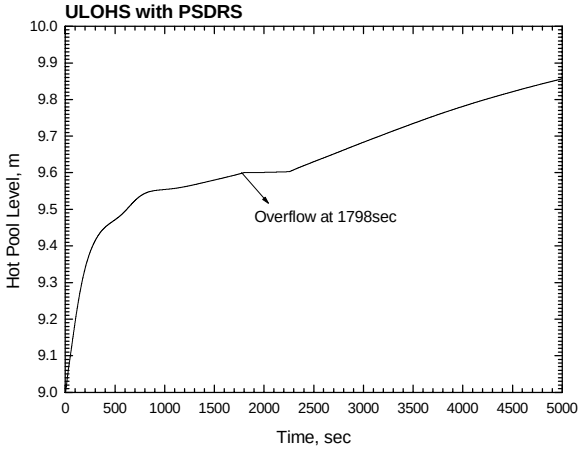

Fig. 14 Hot pool level

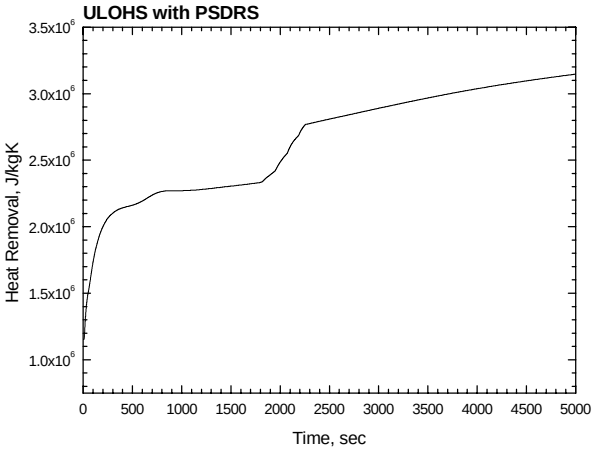

Fig. 15 Heat removal by PSDRS

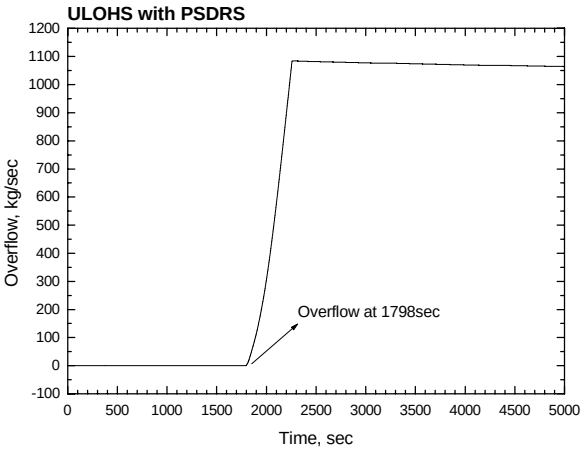

Fig. 16 Overflow rate of hot pool sodium

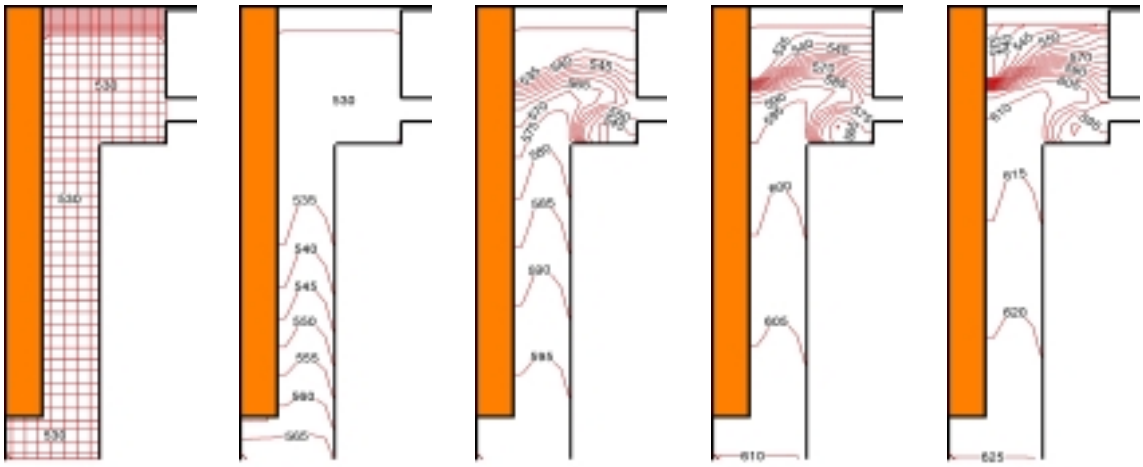

0 sec 30 sec 60 sec 80 sec 110 sec

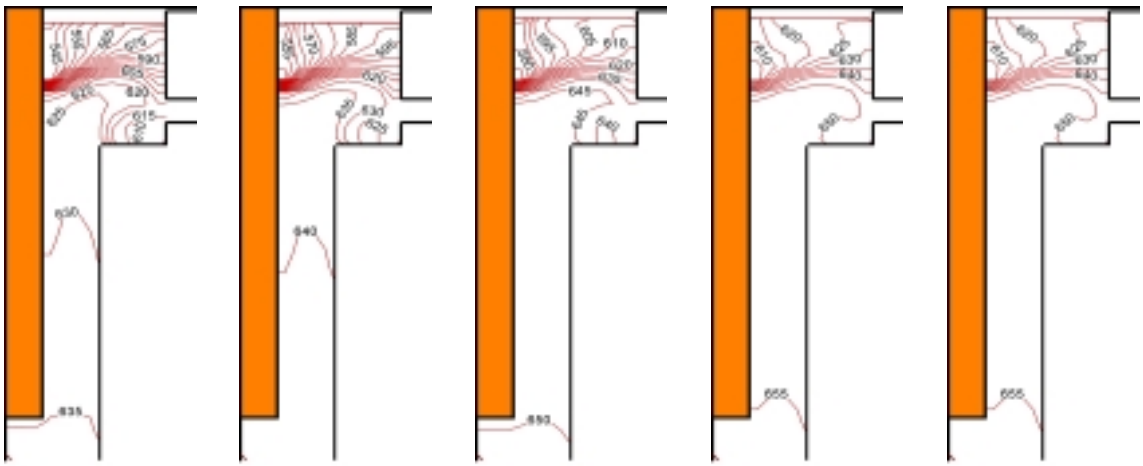

140 sec 170 sec 220 sec 280 sec 400 sec

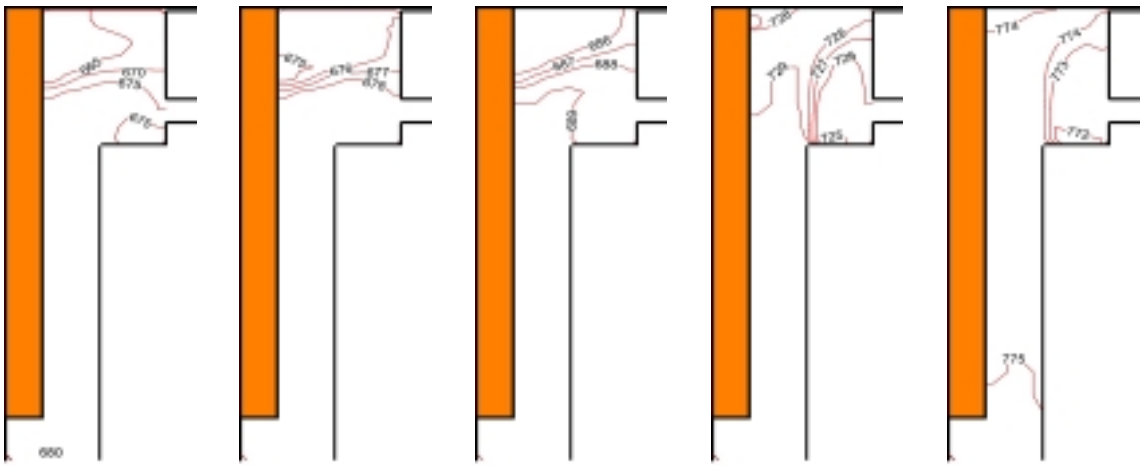

700 sec 900 sec 1800 sec 3000 sec 5000 sec

Fig. 17 Temperature profiles in the hot pool

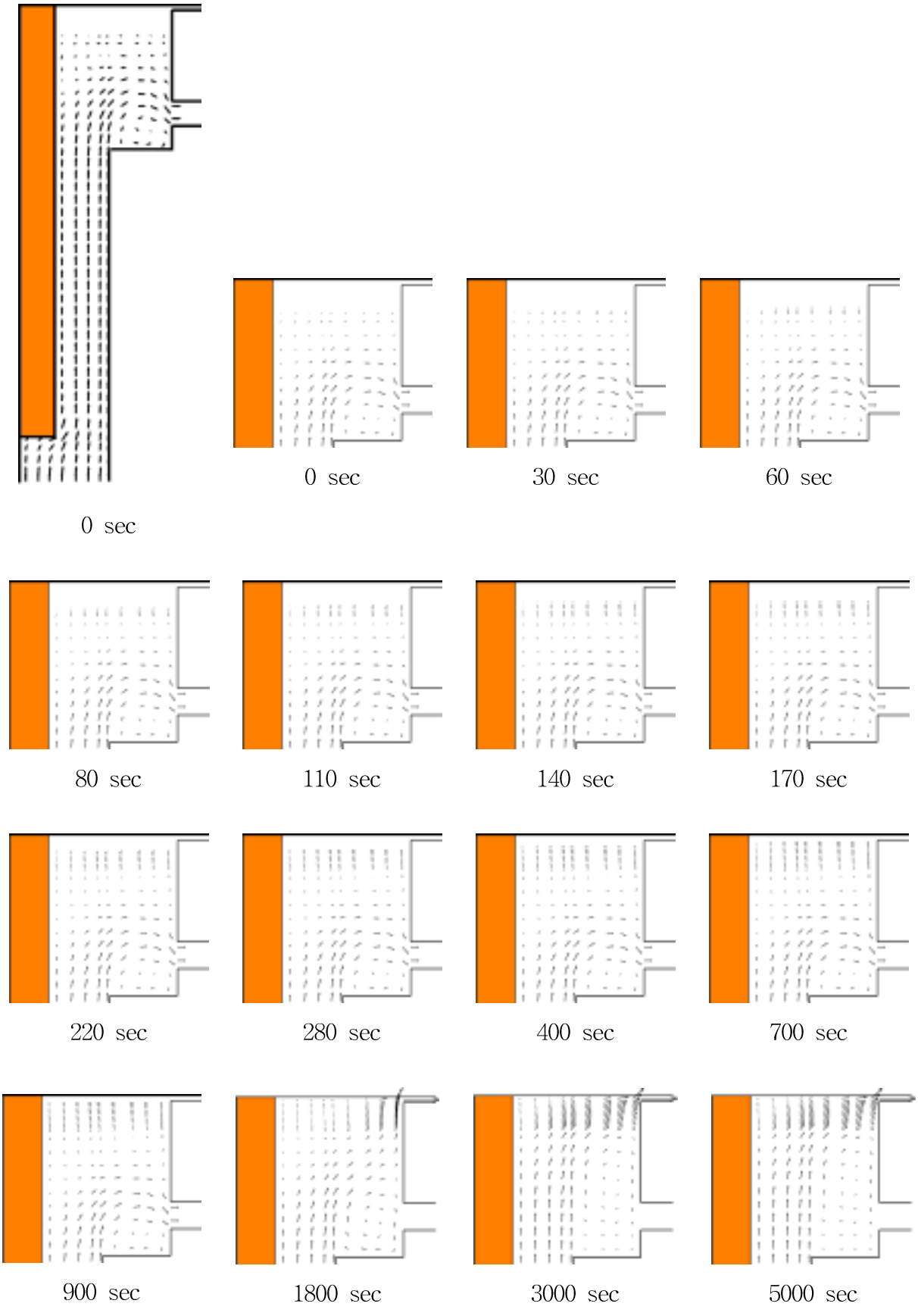

Fig. 18 Velocity profiles in the hot pool

References

[1] A.K. Agrawal et at., An Advanced Thermohydraulic Simulation Code for Transients in LMFBRs (SSC-L Code), BNL-NUREG-50773, Brookhaven Natinal Laboratory, 1973.

[2] C.K. Park et al., KALIMER Design Concept Report, KAERI/TR-888/97, 1997.

[3] J. Zhu, A Low-Diffusive and Oscillation Free Convection Schemes, Communications in Applied Numerical Methods, Vol. 7, pp. 225-232, 1991.

[4] Y.B. Lee et al., Development of the Two-Dimensional Hot Pool Model for Pool-Type Liquid Metal Reactors, Proceedings of the KNS Spring Meeting, 2000.

[5] C.M. Rhie and W. L. Chow, Numerical Study of the Turbulent Flow Past an Airfoil with Trailing Edge Separation, AIAA Journal, Vol. 21, pp. 1525-1532, 1983.

[6] S. Majumdar, Role of Under-relaxation in Momentum Interpolation for Calculation of Flow with Nonstaggered Grids, Numerical Heat Transfer, Vol. 13, pp. 125-132, 1988.

[7] S. K. Choi, Note on the Use of Momentum Interpolation Method for Unsteady Flows, Numerical Heat Transfer, Part A, Vol. 36, pp. 545-550, 1999.

[8] J. P. Van Doormal and G. D. Raithby, Enhancements of the SIMPLE Method for Predicting Incompressible Fluid Flows, Numerical Heat Transfer, Vol. 7, pp. 147-163, 1984.

[9] H. L. Stone, Iterative Solution of Implicit Approximations of Multi-dimensional Partial Differential Equations, SIAM Journal of Numerical Analysis, Vol. 5, pp. 530-558, 1968.

[10] M. H. Wi et al., Study on Thermal-Hydraulic Phenomena in the Upper Plenum of Liquid Metal Fast Breeder Reactor after the Scram by SSC-L Code, PNC ZN9410, 98-025, 1998.

[11] K. Tomorani, et al., Experimental Study on Thermal Stratification in a Reactor Hot Plenum of Japanese Demonstration LMFBR, Proc. 8th International Meeting on Nuclear Reactor Thermal Hydraulic, Sep. 1997.